JOC Article
pubs.acs.org/joc

Multiple Hindered Rotators in a Gyroscope-Inspired Tribenzylamine Hemicryptophane

Najat S. Khan,† Jose Manuel Perez-Aguilar,† Tara Kaufmann, P. Aru Hill, Olena Taratula, One-Sun Lee, Patrick J. Carroll, Jeffery G. Saven,* and Ivan J. Dmochowski*

Department of Chemistry, University of Pennsylvania, Philadelphia, Pennsylvania 19104. †These authors contributed equally to this work.

ivandmo@sas.upenn.edu; saven@sas.upenn.edu

Received December 15, 2010

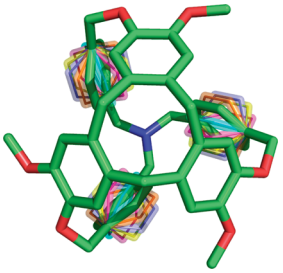

A gyroscope-inspired tribenzylamine hemicryptophane provides a vehicle for exploring the structure and properties of multiple *p*-phenylene rotators within one molecule. The hemicryptophane was synthesized in three steps in good overall yield using mild conditions. Three rotator-forming linkers were cyclized to form a rigid cyclotriveratrylene (CTV) stator framework, which was then closed with an amine. The gyroscope-like molecule was characterized by ^{1}H NMR and ^{13}C NMR spectroscopy, and the structure was solved by X-ray crystallography. The rigidity of the two-component CTV-trismethylamine stator was investigated by ^{1}H variable-temperature (VT) NMR experiments and molecular dynamics simulations. These techniques identified gyration of the three *p*-phenylene rotators on the millisecond time scale at −93 °C, with more dynamic but still hindered motion at room temperature (27 °C). The activation energy for the *p*-phenylene rotation was determined to be ∼10 kcal mol^{-1}. Due to the propeller arrangement of the *p*-phenylenes, their rotation is hindered but not strongly correlated. The compact size, simple synthetic route, and molecular motions of this gyroscope-inspired tribenzylamine hemicryptophane make it an attractive starting point for controlling the direction and coupling of rotators within molecular systems.

Introduction

Synthetic chemical systems provide means to explore complex phenomena in biological machines[1−8] and also to create novel molecular mechanical components.[9] Designs based on macroscopic devices include brakes, gears, propellers, ratchets, turnstiles, rotors, scissors, and most recently gyroscopes.[3,10−14] These molecular systems have been studied extensively in both solution and solid phases as well as on surfaces and in polymers.[15] One challenge in designing these systems is the required restriction of some molecular degrees

(1) Boyer, P. D. *Biosci. Rep.* **1998**, *18*, 97–117.
(2) Elston, T.; Wang, H.; Oster, G. *Nature* **1998**, *391*, 510–513.
(3) Kelly, T. R.; Sestelo, J. P. *Struct. Bonding* (*Berlin*) **2001**, *99*, 19–53.
(4) Nakanishi-Matsui, M.; Sekiya, M.; Nakamoto, R. K.; Futai, M. *Biochim. Biophys. Acta* **2010**, *1797*, 1343–1352.
(5) Rice, S.; Lin, A. W.; Safer, D.; Hart, C. L.; Naber, N.; Carragher, B. O.; Cain, S. M.; Pechatnikova, E.; Wilson-Kubalek, E. M.; Whittaker, M.; Pate, E.; Cooke, R.; Taylor, E. W.; Milligan, R. A.; Vale, R. D. *Nature* **1999**, *402*, 778–784.
(6) Sindelar, C. V.; Downing, K. H. *Proc. Natl. Acad. Sci. U.S.A.* **2010**, *107*, 4111–4116.
(7) Terashima, H.; Kojima, S.; Homma, M. *Int. Rev. Cell. Mol. Biol.* **2008**, *270*, 39–85.
(8) Woolley, D. M. *Biol. Rev. Camb. Philos. Soc.* **2010**, *85*, 453–470.
(9) Kay, E. R.; Leigh, D. A.; Zerbetto, F. *Angew. Chem., Int. Ed.* **2007**, *46*, 72–191.
(10) Day, A. I.; Blanch, R. J.; Arnold, A. P.; Lorenzo, S.; Lewis, G. R.; Dance, I. *Angew. Chem., Int. Ed.* **2002**, *41*, 275–277.
(11) Garcia-Garibay, M. A. *Proc. Natl. Acad. Sci. U.S.A.* **2005**, *102*, 10771–10776.
(12) Iwamura, H.; Mislow, K. *Acc. Chem. Res.* **1988**, *21*, 175–182.
(13) Michl, J.; Sykes, C. H. *ACS Nano* **2009**, *3*, 1042–1048.
(14) Skopek, K.; Hershberger, M. C.; Gladysz, J. A. *Coord. Chem. Rev.* **2007**, *251*, 1723–1733.

Published on Web 01/27/2011 DOI: 10.1021/jo102480s

SCHEME 1. Gyroscope-Inspired Tribenzylamine Hemicryptophane (5) Possessing a Rigid Stator (a and c) and Three Rotator Groups (b)[a]

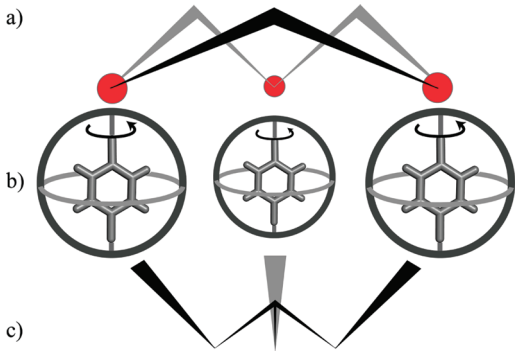

[a]Arrows illustrate rotation but are not intended to suggest unidirectionality.

of freedom, while allowing the specific motions of targeted molecular components.[9] Although synthesis of such molecules can also be challenging, criteria for the construction of molecular gyroscopes have been identified and generally applied: rotary elements (rotators) are attached to a static framework (stator); steric contacts, internal rotation barriers, and interaction with solvent should be minimized to allow low-friction, low-barrier rotary motion; rotating groups are isolated and/or well-separated from each other. To expand upon these criteria, we designed a gyroscope-inspired framework with cyclotriveratrylene (CTV) and trismethylamine as the two-component stator, bridged by three *p*-phenylene rotators (Scheme 1). Previously, two opposing CTV units have been linked to generate cryptophanes with suitable cavities for host−guest chemistry, as well as useful biosensing and chiroptical properties.[16−31] CTV has also been employed in supramolecular assemblies, gels, and organic microporous polymers.[32] In the current design, a single CTV unit provides a rigid hemicryptophane framework for the synthesis of a novel gyroscope-inspired molecule. Our design incorporates a novel combination of features: (i) an efficient, high-yielding synthetic scheme, (ii) multiple, proximate rotators in one covalently bonded molecular system, (iii) exclusion of other molecules and ions from the stator interior that may impede rotator motion, and (iv) hindered rotators experiencing friction through exposure to solvent.

Gyroscope-inspired molecular systems have focused largely on approaching barrierless rotation of isolated or sequestered rotors. One of the first examples (also referred to as a molecular turnstile) was synthesized by Moore and Bedard.[33,34] The creative design included a rigid hexakis-(phenylacetylene) framework that preserved the low barrier of rotation about the 1,4-axis of the substituted *p*-phenylene moiety. Garcia-Garibay and co-workers extended these ideas in the construction of amphidynamic crystals,[11,15,35−54] where the introduction of bulky substituents creates sufficient space in the lattice framework to allow near-barrierless rotation of the central *p*-phenylene group. Furthermore, the *p*-phenylene moiety can be functionalized to create a dipole moment that could be used for controlling motion with an external electric field.[11,36−38,42] Following a different approach, Gladysz and co-workers prepared a series of metal-centered molecular gyroscopes in which the rotator is protected by three-spoke structures as part of the stator. The rotational dynamics of these gyroscopes were studied in solution, and their crystal structures indicated sufficient free volume around the rotator to allow

(15) Karlen, S. D.; Godinez, C. E.; Garcia-Garibay, M. A. *Org. Lett.* **2006**, *8*, 3417–3420.
(16) Bartik, K; L., M.; Dutasta, J. P.; Collet, A; Reisse, J. *J. Am. Chem. Soc.* **1998**, *120*, 784–791.
(17) Brotin, T.; Dutasta, J. P. *Eur. J. Org. Chem.* **2003**, *6*, 973–984.
(18) Brotin, T.; Roy, V.; Dutasta, J. P. *J. Org. Chem.* **2005**, *70*, 6187–6195.
(19) Chambers, J. M.; Hill, P. A.; Aaron, J. A.; Han, Z.; Christianson, D. W.; Kuzma, N. N.; Dmochowski, I. J. *J. Am. Chem. Soc.* **2009**, *131*, 563–569.
(20) Collet, A. *Comp. Supramol. Chem. 2* **1996**, 325–365.
(21) Fogarty, H. A.; Berthault, P.; Brotin, T.; Huber, G.; Desvaux, H.; Dutasta, J. P. *J. Am. Chem. Soc.* **2007**, *129*, 10332–10333.
(22) Gautier, A.; Mulatier, J. C.; Crassous, J.; Dutasta, J. P. *Org. Lett.* **2005**, *7*, 1207–1210.
(23) Gosse, I.; Dutasta, J. P.; Perrin, M.; Thozet, A. *New J. Chem.* **1999**, *23*, 545–548.
(24) Hill, P. A.; Wei, Q.; Eckenhoff, R. G.; Dmochowski, I. J. *J. Am. Chem. Soc.* **2007**, *129*, 9262–9263.
(25) Hill, P. A.; Wei, Q.; Troxler, T.; Dmochowski, I. J. *J. Am. Chem. Soc.* **2009**, *131*, 3069–3077.
(26) Martinez, A.; Robert, V.; Gornitzka, H.; Dutasta, J. P. *Chem. Eur. J.* **2010**, *16*, 520–527.
(27) Mynar, J. L.; Lowery, T. J.; Wemmer, D. E.; Pines, A.; Frechet, J. M. *J. Am. Chem. Soc.* **2006**, *128*, 6334–6335.
(28) Schlundt, A.; Kilian, W.; Beyermann, M.; Sticht, J.; Guenther, S.; Höpner, S.; Falk, K.; Roetzschke, O.; Mitschang, L.; Freund, C. *Angew. Chem.* **2009**, *121*, 4206–4209.
(29) Seward, G. K.; Wei, Q.; Dmochowski, I. J. *Bioconjug. Chem.* **2008**, *19*, 2129–2135.
(30) Spence, M. M.; Rubin, S. M.; Dimitrov, I. E. *Proc. Natl. Acad. Sci. U.S.A.* **2001**, *98*, 10654–10657.
(31) Wei, Q.; Seward, G. K.; Hill, P. A.; Patton, B.; Dimitrov, I. E.; Kuzma, N. N.; Dmochowski, I. J. *J. Am. Chem. Soc.* **2006**, *128*, 13274–13283.
(32) Hardie, M. J. *Chem. Soc. Rev.* **2010**, *39*, 516–527.
(33) Kottas, G. S.; Clarke, L. I.; Horinek, D.; Michl, J. *Chem. Rev.* **2005**, *105*, 1281–1376.
(34) Moore, J. S.; Bedard, T. C. *J. Am. Chem. Soc.* **1995**, *117*, 10662–10671.
(35) Cizmeciyan, D.; Yonutas, H.; Karlen, S. D.; Garcia-Garibay, M. A. *Solid State Nucl. Magn. Reson.* **2005**, *28*, 1–8.
(36) Dominguez, Z.; Dang, H.; Strouse, M. J.; Garcia-Garibay, M. A. *J. Am. Chem. Soc.* **2002**, *124*, 7719–7727.
(37) Dominguez, Z.; Dang, H.; Strouse, M. J.; Garcia-Garibay, M. A. *J. Am. Chem. Soc.* **2002**, *124*, 2398–2399.
(38) Dominguez, Z.; Khuong, T. A.; Dang, H.; Sanrame, C. N.; Nunez, J. E.; Garcia-Garibay, M. A. *J. Am. Chem. Soc.* **2003**, *125*, 8827–8837.
(39) Garcia-Garibay, M. A. *Angew. Chem., Int. Ed.* **2007**, *46*, 8945–8947.
(40) Garcia-Garibay, M. A. *Nat. Mater.* **2008**, *7*, 431–432.
(41) Garcia-Garibay, M. A.; Dang, H. *Org. Biomol. Chem.* **2009**, *7*, 1106–1114.
(42) Godinez, C. E.; Zepeda, G.; Garcia-Garibay, M. A. *J. Am. Chem. Soc.* **2002**, *124*, 4701–4707.
(43) Godinez, C. E.; Zepeda, G.; Mortko, C. J.; Dang, H.; Garcia-Garibay, M. A. *J. Org. Chem.* **2004**, *69*, 1652–1662.
(44) Gould, S. L.; Tranchemontagne, D.; Yaghi, O. M.; Garcia-Garibay, M. A. *J. Am. Chem. Soc.* **2008**, *130*, 3246–3247.
(45) Jarowski, P. D.; Houk, K. N.; Garcia-Garibay, M. A. *J. Am. Chem. Soc.* **2007**, *129*, 3110–3117.
(46) Karlen, S. D.; Garcia-Garibay, M. A. *Chem. Commun.* **2005**, 189–191.
(47) Karlen, S. D.; Ortiz, R.; Chapman, O. L.; Garcia-Garibay, M. A. *J. Am. Chem. Soc.* **2005**, *127*, 6554–6555.
(48) Khuong, T. A.; Dang, H.; Jarowski, P. D.; Maverick, E. F.; Garcia-Garibay, M. A. *J. Am. Chem. Soc.* **2007**, *129*, 839–845.
(49) Khuong, T. A.; Nunez, J. E.; Godinez, C. E.; Garcia-Garibay, M. A. *Acc. Chem. Res.* **2006**, *39*, 413–422.
(50) Kuzmanich, G.; Natarajan, A.; Chin, K. K.; Veerman, M.; Mortko, C. J.; Garcia-Garibay, M. A. *J. Am. Chem. Soc.* **2008**, *130*, 1140–1141.
(51) Nunez, J. E.; Natarajan, A.; Khan, S. I.; Garcia-Garibay, M. A. *Org. Lett.* **2007**, *9*, 3559–3561.
(52) O'Brien, Z. J.; Karlen, S. D.; Khan, S.; Garcia-Garibay, M. A. *J. Org. Chem.* **2010**, *75*, 2482–2491.
(53) Rodriguez-Molina, B.; Ochoa, M. E.; Farfan, N.; Santillan, R.; Garcia-Garibay, M. A. *J. Org. Chem.* **2009**, *74*, 8554–8565.
(54) Rodriguez-Molina, B.; Pozos, A.; Cruz, R.; Romero, M.; Flores, B.; Farfan, N.; Santillan, R.; Garcia-Garibay, M. A. *Org. Biomol. Chem.* **2010**, *8*, 2993–3000.

SCHEME 2. Three-Step Synthesis of Gyroscope-Inspired Tribenzylamine Hemicryptophane 5

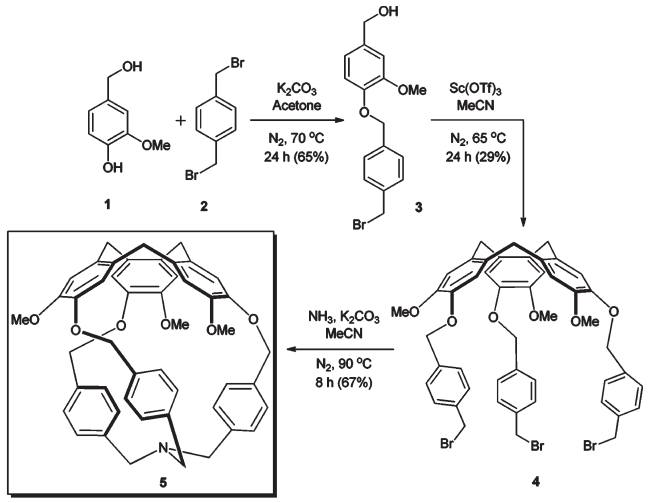

Overall Yield (3 steps) = 13%

low-barrier rotation.[9,55−59] Most recently, Kitagawa et al. designed a self-assembled supramolecular gyroscope where the stator is a heterocapsule formed by noncovalent interactions and the rotator is an encapsulated guest.[60]

Herein, we report a streamlined synthesis of a gyroscope-inspired tribenzylamine hemicryptophane (**5**; Scheme 2) involving multiple hindered rotators, where fast rotation is observed by ^{1}H NMR spectroscopy above a critical temperature. Rotations about the 1,4-axis of the three *p*-phenylene rotators encased in a rigid CTV-trismethylamine stator were investigated using ^{1}H variable-temperature (VT) NMR spectroscopy and molecular dynamics (MD) simulations.

Results and Discussion

Synthesis and X-ray Crystal Structure of Hemicryptophane 5. In order to synthesize the gyroscope-inspired tribenzylamine hemicrytophane **5**, the linkers (including the rotators) were first cyclized in the rigid CTV framework and then closed with an amine to form the final three-dimensional structure (Scheme 2). Reaction of commercially available vanillyl alcohol **1** and dibromo-*p*-xylene **2** gave the versatile linker **3** in 65% yield. Cyclization of **3** was achieved with a catalytic amount of $Sc(OTf)_3$ in acetonitrile to afford the "gyroscope scaffold intermediate" **4** in 29% yield. This reaction was based on previous protocols where various 3,4-disubstituted benzyl alcohols were treated with catalytic $Sc(OTf)_3$ to prepare CTV and cryptophane derivatives.[18] Compound **4** was reacted with 7 N NH_3 in MeOH to give **5** in 67% yield, with an overall yield of 13% for the three steps. Compound **5** was characterized by solution ^{1}H NMR and ^{13}C NMR spectroscopy, high-resolution mass spectrometry (using the electrospray ionization method), and X-ray crystallography. This short synthetic scheme utilizes mild conditions and results in high overall yields. Moreover, this route provides ample versatility by increasing the number of methylene spacer units or introducing new functional groups on **3** to form rotators with different conformations, rotation barriers, and dipole moments.

The X-ray crystal structure of **5** indicates the three rotators adopt a propeller conformation (Figure 1). **5** crystallizes in the monoclinic space group $P2_1/c$, and each unit cell consists of four molecules with two of each enantiomer (Figure 1; Figure S1, Supporting Information). In both enantiomers the *p*-phenylene rotators are oriented edgewise into the interior (angled away from the methoxy group *ortho* to them) with an average dihedral angle of ~88.1° for $O-C_{benzylic}-C_{phenyl}-C_{phenyl}$, ~ −68.6° for $N-C_{benzylic}-C_{phenyl}-C_{interior\text{-}phenyl}$, and ~107.5° for $N-C_{benzylic}-C_{phenyl}-C_{exterior\text{-}phenyl}$ (see Figure 1c). The minimal distance from the phenylic proton on C44 (pointing into the cage) to the plane described by the next aryl ring (C10−C15) is relatively small at 3.22 Å. After the van der Waals radii for hydrogen and carbon are included,[61] the "clearance" distance is approximately 0.32 Å. The distance from the same proton to the nitrogen atom was even shorter at 2.97 Å, with a clearance distance of 0.22 Å when van der Waals radii are included, as the nitrogen is oriented into the interior with an average C−N−C bond angle of 114.42° (see Figure 1c). This propeller-shaped conformation with a pyramidal nitrogen atom where the lone pair is pointed into the cage is similar to the crystal structure of tribenzylamine, where the rigid CTV is not present.[62] It is believed that this conformation is primarily favored due to steric hindrance.[62] Despite the propeller conformation of the rotators and the positioning of the nitrogen atom into the interior of the cage, rotator motion is expected, given the observed clearance distances (Figure 1).

Unlike some previously reported porous gyroscopes,[58] which encountered barriers to rotation due to the intercalation of solvent molecules (or neighboring molecules in solid state), the small internal volume in **5** should prevent guest encapsulation. Indeed, X-ray crystallography indicated an empty tribenzylamine hemicryptophane, lacking solvent molecules. Small molecules such as helium, dihydrogen, dinitrogen, and xenon were not observed to bind to **5** at 1 atm over a range of temperatures, +47 to −93 °C (see the Supporting Information for experimental details). Molecular dynamics simulations were also in agreement with the experimental findings and suggest that these small molecular species should be excluded from the interior (Figure S2, Supporting Information). Computational modeling was used to explore effects due to rotation of the *p*-phenylene rotators. GRASP[63] was employed in order to investigate whether a potential interior cavity within **5** emerges with rotation of the rotators. With a probe radius of 1.4 Å, only in improbable, high-energy structures (ΔE > 30 kcal mol^{-1}, where ΔE is the energy relative to the X-ray structure) where the angle of each *p*-phenylene rotator increased by 90° relative

(55) Nawara, A. J.; Shima, T.; Hampel, F.; Gladysz, J. A. *J. Am. Chem. Soc.* **2006**, *128*, 4962–4963.
(56) Shima, T.; Hampel, F.; Gladysz, J. A. *Angew. Chem., Int. Ed.* **2004**, *43*, 5537–5540.
(57) Skopek, K.; Barbasiewicz, M.; Hampel, F.; Gladysz, J. A. *Inorg. Chem.* **2008**, *47*, 3474–3476.
(58) Wang, L.; Hampel, F.; Gladysz, J. A. *Angew. Chem., Int. Ed.* **2006**, *45*, 4372–4375.
(59) Wang, L.; Shima, T.; Hampel, F.; Gladysz, J. A. *Chem. Commun.* **2006**, 4075–4077.
(60) Kitagawa, H.; Kobori, Y.; Yamanaka, M.; Yoza, K.; Kobayashi, K. *Proc. Natl. Acad. Sci. U.S.A.* **2009**, *106*, 10444–10448.
(61) Bondi, A. *J. Phys. Chem.* **1964**, *68*, 441–451.
(62) Iwasaki, F. *Acta Crystallogr.* **1972**, *B28*, 3370–3376.
(63) Nicholls, A.; Sharp, K. A.; Honig, B. *Proteins* **1991**, *11*, 281–296.

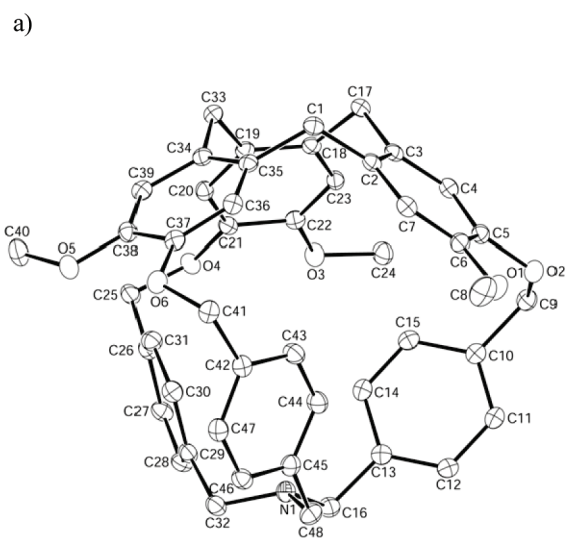

N1-C32	1.466 (2) Å	C28-C29-C32-N1	97.7 (2)°
N1-C48	1.464 (2) Å	O2-C9-C10-C11	-90.9 (2)°
N1-C16	1.461 (2) Å	O6-C41-C42-C47	-89.1 (2)°
C32-C29	1.509 (2) Å	O4-C25-C26-C27	-83.1 (2)°
C48-C45	1.512 (3) Å	C14-C13-C16-N1	-61.5 (2)°
C16-C13	1.514 (3) Å	C13-C16-N1-C48	-84.9 (2)°
C32-N1-C48	114.84 (14)°	C30-C29-C32-N1	-77.7 (2)°
C48-N1-C16	113.96 (14)°	C29-C32-N1-C16	-75.4 (2)°
C32-N1-C16	114.45 (14)°	C44-C45-C48-N1	-66.6 (2)°
N1-C32-C29	108.93 (14)°	C45-C48-N1-C32	-79.4 (2)°
N1-C48-C45	109.15 (14)°	C12-C13-C16-N1	117.2 (2)°
N1-C16-C13	110.18 (14)°	C46-C45-C48-N1	107.6 (2)°
O2-C9-C10-C15	86.1 (2)°	C13-C16-N1-C32	140.2 (2)°
O6-C41-C42-C43	85.4 (2)°	C29-C32-N1-C48	150.05 (13)°
O4-C25-C26-C31	93.8 (2)°	C45-C48-N1-C16	145.83 (14)°

FIGURE 1. (a) ORTEP representations for **5** with atom labels. Hydrogen atoms are omitted for clarity. (b) Space-filling side and bottom view of **5**. Atom color code: C is gray, O is red, N is blue, and H is white. (c) Selected bond lengths (Å), angles (deg), and dihedral angles (deg) of compound **5**.

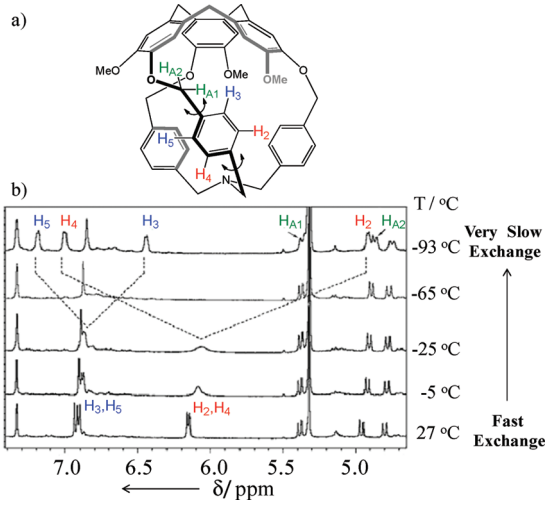

FIGURE 2. (a) Schematic model of the molecular motion of **5**. (b) ^{1}H VT-NMR spectra of **5** measured in CD_2Cl_2 with a 500 MHz spectrometer.

to the crystal structure was a cavity identified (Figure S3, Supporting Information). This suggests that a cavity of sufficient volume to accommodate small guest molecules is essentially nonexistent, thereby preventing the inclusion of small molecules that may hinder *p*-phenylene rotation.

^{1}H VT-NMR Experiments with Hemicryptophane 5. In order to investigate the energy barrier of the rotators in solution phase, we performed a ^{1}H VT-NMR study of **5** in CD_2Cl_2 from −93 to +27 °C. The NMR spectra in Figure 2 indicate that the rotational rate of the *p*-phenylene rotators became slow on the NMR time scale as the temperature was decreased. At 27 °C, the four protons (labeled H_2, H_3, H_4, and H_5 in Figure 2a) on each of the three rotators were split into two doublets at 6.1 ppm (average signal from H_2 and H_4) and 6.9 ppm (average signal from H_3 and H_5). Upon cooling, these doublets became broader and the energy barrier for *p*-phenylene rotation was estimated from eqs 1 and 2[64] (see the Experimental Procedures) to be 9.2 kcal mol^{-1} from the coalescence temperature (ca. −70 °C; $k_{coalesce} \sim 2300$ Hz). As the temperature was further reduced to −93 °C, a new pair of doublets of equal intensity (three protons each) arose for each doublet that coalesced. This led to splitting of the doublet for H_2 and H_5 and also H_3 and H_4, where H_2 and H_3 shift upfield as they are pointed into the cavity while H_4 and H_5 are oriented away from the cavity. The H_3-H_5 splitting pattern (Figure 2b) shows that *p*-phenylene rotation at −93 °C is slow on the NMR time scale, $t_{rot} > 3$ ms. Similar temperature-dependent behavior was recently reported for a 2,3-dichlorophenylene rotator caged within a polysilaalkane stator.[65] In line with our design, the stator remained rigid throughout the ^{1}H VT-NMR data set, as indicated by the fact that the integration and splitting pattern of all CTV-trismethylamine proton peaks were constant. It is also interesting to note that protons H_{A1} and H_{A2} remained diastereotopic throughout the ^{1}H VT-NMR series (Figure 2b). All peaks were assigned by ^{1}H−^{1}H NOESY experiments (Figure 3).

Molecular Dynamics Simulations. To investigate the conformational fluctuations of the rotators and stator, MD simulations were carried out on **5** (Figure 4). One of the crystal structures was used as the initial structure, and the length of the simulations was 50 ns. Equilibration was confirmed by monitoring relaxation of structural parameters (Figure S4, Supporting Information). Three dihedral angles that reflect the conformations of the rotators were selected: ($\alpha \equiv$ N1−C16−C13−C14, $\beta \equiv$ N1−C32−C29−C30, and $\gamma \equiv$ N1−C48−C45−C44). The symmetry of the structure yields nearly identical average values of these angles that are in agreement with the values observed in the crystal structure: $\alpha = -72.3 \pm 10°$, $\beta = -71.8 \pm 10°$, and $\gamma = -72.8 \pm 10°$; the uncertainties

(64) Sandstrom, J. *Dynamic NMR Spectroscopy*; Academic Press: New York, 1983.
(65) Setaka, W.; Ohmizu, S.; Kira, M. *Chem. Lett.* **2010**, *39*, 468–469.

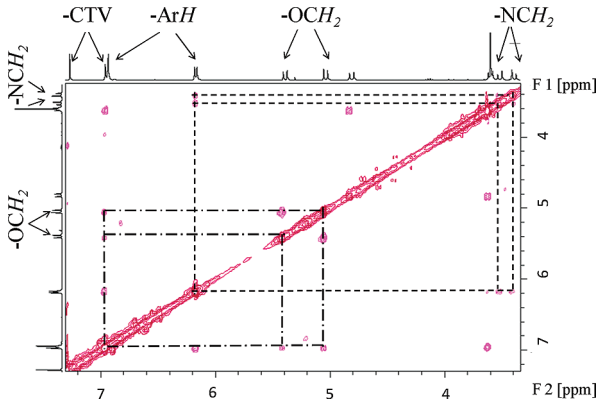

FIGURE 3. $^1H-^1H$ NOESY spectrum of **5** in $CDCl_3$ at 27 °C measured with a 500 MHz spectrometer to determine the assignment of protons.

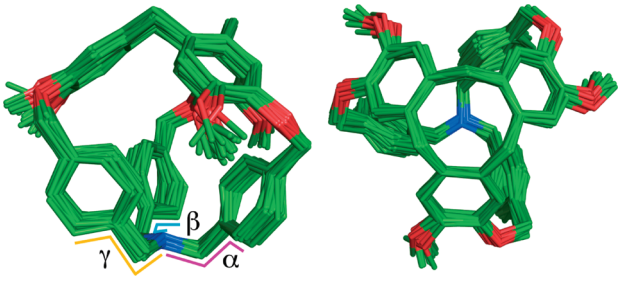

FIGURE 4. Orthogonal views of 30 superimposed structures from the MD simulation of **5**. The dihedral angles are indicated: α (magenta), *β* (cyan), and *γ* (yellow).

(fluctuations) are one standard deviation (Figure S5, Supporting Information). The MD simulations at 25 °C indicated limited fluctuations within the structure on the nanosecond time scale (Figure 4), and the CTV unit that forms the stator remains highly rigid, in agreement with the NMR results noted above. The *p*-phenylene units are not observed to rotate and instead librate in a manner consistent with a hindered rotor that rotates on a time scale >100 ns. Therefore, simulations, X-ray, and NMR structural data all agree that the propeller-shaped conformation is highly favored in **5**. High temperatures were artificially employed to observe rotation in the simulations: at 527 °C, rotations of the three *p*-phenylenes are frequent, conformations where the rotators are directed edgewise into the interior (similar to what is seen in the crystal structure) are preferentially populated, and no preferred rotational direction in the three *p*-phenylenes is observed.

To investigate further the *p*-phenylene rotation and interactions among the rotators, the crystal structure of **5** was minimized, and the dihedral angle α was systematically varied (Figure 5). The structure was then relaxed via energy minimization, constraining the coordinates of all atoms but those in the two remaining *β* and *γ* *p*-phenylene rings. The *β* ring is essentially invariant during the rotation. The *γ* ring only rotates at most 19.7° to accommodate the 180° rotation of the α ring. An energy barrier arises due to this interaction between the α ring and *γ* ring. Interestingly, the rotational energy barrier estimated from this simplistic and highly constrained calculation (~12 kcal mol^{-1}) is consistent with the experimental value inferred from the ^1H VT-NMR

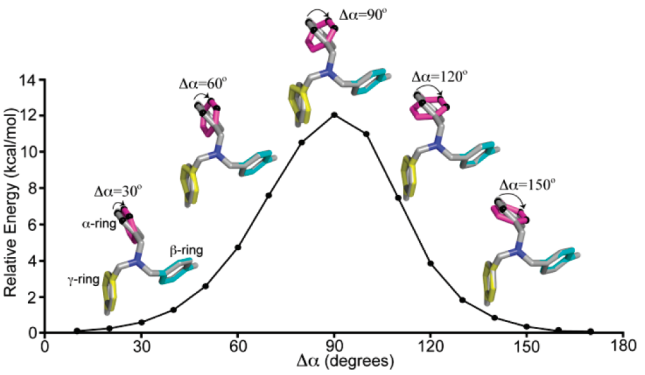

FIGURE 5. Minimized energy as a function of Δα, which is rotation of the α dihedral angle relative to the energy-minimized X-ray structure (gray). The crystal structure of **5** was minimized, and the angle α was varied in 10° increments, driving rotation of the α ring (magenta). For each value of Δα, the structure was energy minimized, constraining the coordinates of all atoms but those in the two remaining *p*-phenylene rotators: *β* ring (cyan) and *γ* ring (yellow). For clarity, the CTV moiety and hydrogens are not shown; two carbons of the α ring are rendered in black.

experiments (~10 kcal mol^{-1}). The modeling results suggest that, although not entirely independent, the rotations of the α and *γ* rings are only weakly coupled.

Conclusions

In summary, the novel gyroscope-inspired tribenzylamine hemicryptophane **5** was synthesized in three steps in good overall yield using mild conditions. This synthetic route offers the possibility of preparing hemicryptophanes with multiple, proximate rotators, where the molecular properties of the rotators can be varied by changing the length and composition of the linkers used to cyclize the "gyroscope scaffold intermediate" **4**. The compact size of the cavity in this system helps to avoid the inclusion of solvent and gaseous molecules that have the potential to inhibit rotation. ^1H VT-NMR data indicate a critical temperature for the onset of rotation on the submillisecond time scale and a hindered, dynamic motion of these three rotators at room temperature. The desired rigidity of the CTV stator and the rotator properties of the *p*-phenylenes were corroborated by ^1H VT-NMR spectroscopy and MD simulations. As a *p*-phenylene ring rotates, it encounters one of the neighboring *p*-phenylenes, leading to a steric barrier that hinders rotation. Rotations of the rings appear not to be strongly correlated with one another.

The compact size and molecular motions of **5** make it a compelling initial motif from which to engineer unidirectional, potentially coupled rotators for molecular locomotion or transmission of torque. Toward this goal, it may be possible to introduce sterically bulky substituents on the linkers to control the temperatures at which rotation becomes accessible and to favor one direction of rotation. Different substituent groups can also be introduced to create a dipole moment on the rotators, thereby allowing the use of electric fields to explore rapid conformational response in these systems and to control the direction of rotation.

Experimental Procedures

Reagents. All reactions were carried out in oven-dried glassware under an atmosphere of dry nitrogen. Column

chromatography was performed using 60 Å porosity, 40−75 μm particle size silica gel from Sorbent Technologies. Thin-layer chromatography (TLC) was performed using silica gel plates with UV light at 254 nm for detection. ^{1}H NMR (360 and 500 MHz) and ^{13}C NMR (125 MHz) spectra were acquired on Bruker DMX 360 and AMX 500 spectrometers. Electrospray ionization (ESI) mass spectrometry was performed in high-resolution mode on a Micromass Autospec instrument. All reagents were commercially available and used without further purification, unless otherwise stated.

[4-((4-(Bromomethyl)benzyl)oxy)-3-methoxyphenyl]methanol (3). A mixture of vanillyl alcohol (**1**; 2.5091 g, 16.276 mmol, 1.0 equiv), dibromo-*p*-xylene (**2**; 6.4033 g, 24.259 mmol, 1.5 equiv), and K_2CO_3 (2.2511 g, 16.288 mmol, 1.0 equiv) dissolved in acetone (24.0 mL, 0.786 g/mL, 18.9 g) was heated at 70 °C overnight with stirring. The reaction solvent was removed by rotary evaporation. The resulting residue was rinsed in a separatory funnel with a 1:1 mixture of H_2O (60 mL) and CH_2Cl_2 (60 mL). The phases were separated, and the aqueous layer was extracted three times with CH_2Cl_2 (100 mL). The combined organic layer was washed once with 1 M NaOH (100 mL) and once with saturated NaCl (100 mL). The organic layer was dried over $MgSO_4$, filtered, and evaporated under reduced pressure. The crude material was purified by silica gel column chromatography (5/95 acetone/CH_2Cl_2 → 20/80 acetone/CH_2Cl_2) to give **3** as a white powder (3.5422 g, 65%): mp 86−88 °C; ^{1}H NMR (500 MHz, $CDCl_3$, 25 °C) δ 7.42−7.38 (m, 4H), 6.96 (s, 1H), 6.85−6.81 (m, 2H), 5.14 (s, 2H), 4.60 (s, 2H), 4.49 (s, 2H), 3.89 (s, 3H), 1.86 (s, 1H); ^{13}C NMR (125 MHz, $CDCl_3$, 25 °C) δ 149.9, 147.6, 137.6, 137.5, 134.5, 129.4, 127.7, 119.4, 114.1, 111.1, 70.8, 65.4, 56.1, 33.36; HRMS (ESI) *m*/*z* calcd for $C_{16}H_{17}BrO_3$ ($M+Na^+$) 359.0259, found 359.0239.

2,7,12-Tris((4-(bromomethyl)benzyl)oxy)-3,8,13-trimethoxy-10,15-dihydro-5*H*-tribenzo[*a*,*d*,*g*]cyclononene (4). A mixture of **3** (2.0232 g, 6.0210 mmol, 1.0 equiv) and $Sc(OTf)_3$ (0.0295 g, 0.0599 mmol, 0.01 equiv) dissolved in MeCN (5.9 mL, 0.786 g/mL, 4.7 g) was heated at 65 °C overnight with stirring. The reaction solvent was removed by rotary evaporation. The resulting residue was extracted twice with CH_2Cl_2 (150 mL) and washed three times with saturated NaCl (150 mL). The organic layer was dried over anhydrous $MgSO_4$, filtered, and evaporated under reduced pressure. The crude material was purified by silica gel column chromatography (CH_2Cl_2 → 2/98 THF/CH_2Cl_2) to give **4** as a white powder (0.5571 g, 29%): mp 91−93 °C; ^{1}H NMR (360 MHz, $CDCl_3$, 25 °C) δ 7.39−7.37 (m, 12H), 6.85 (s, 3H), 6.72 (s, 3H), 5.09 (s, 6H), 4.73 (d, 3H, J = 13.7 Hz), 4.50 (s, 6H), 3.76 (s, 9H), 3.50 (d, 3H, J = 13.8 Hz); ^{13}C NMR (125 Hz, $CDCl_3$, 25 °C) δ 148.6, 147.2, 137.9, 137.5, 132.9, 131.9, 129.4, 127.6, 116.4, 114.0, 71.4, 56.4, 36.6, 33.3; HRMS (ESI) m/z calcd for $C_{48}H_{45}Br_3O_6$ (M^+) 954.0766, found 954.0724. The NMR spectra matched the reported literature data.[66]

Tribenzylamine Hemicryptophane (5). A mixture of **4** (0.0406 g, 0.0426 mmol, 1.0 equiv) and K_2CO_3 (0.0869 g, 0.629 mmol, 15.0 equiv) dissolved in MeCN (58 mL, 0.786 g/mL, 46 g) was heated at 90 °C with stirring as 7 N NH_3 in MeOH (0.0711 mL of 7 N NH_3, 0.5 mmol, ∼12 equiv, in 4.7 mL of MeCN) was added by a syringe pump over 8 h. The reaction solvent was removed by rotary evaporation. The resulting residue was extracted with CH_2Cl_2 and transferred to a separatory funnel. The organic layer was washed once with a 1/1 mixture of H_2O (50 mL) and 1 M NaOH (50 mL) and then with 1 M NaOH (50 mL). The aqueous layer was extracted with CH_2Cl_2 (50 mL), and the combined organic layer was washed with saturated NaCl (50 mL). The organic layer was dried over anhydrous $MgSO_4$, filtered, and evaporated under reduced pressure. The crude material was purified by silica gel column chromatography (50/50 CH_2Cl_2/hexanes → 50/40/10 CH_2Cl_2/hexanes/EtOAc → 60/30/10 CH_2Cl_2/hexanes/EtOAc; all with 1% TEA) to give **5** as a white powder (0.0206 g, 67%): mp > 250 °C dec; ^{1}H NMR (360 MHz, $CDCl_3$, 25 °C) δ 7.34 (s, 3H), 6.96−6.93 (m, 9H), 6.18 (d, 6H, J = 7.9 Hz), 5.41 (d, 3H, J = 12.1 Hz), 5.06 (d, 3H, J = 12.2 Hz), 4.83 (d, 3H, J = 13.7 Hz), 3.60 (d, 3H, J = 13.8 Hz), 3.58 (s, 9H), 3.54 (d, 3H, J = 13.2 Hz), 3.41 (d, 3H, J = 13.2 Hz); ^{13}C NMR (125 MHz, $CDCl_3$, 25 °C) δ 147.7, 143.0, 140.3, 132.9, 131.7, 130.8, 128.4, 127.4, 117.9, 113.9, 68.8, 55.5, 55.3, 34.9; HRMS (ESI) *m*/*z* calcd for $C_{48}H_{45}NO_6$ ($M + H^+$) 732.3326, found 732.3340.

Crystal Growth and X-ray Crystallography. Compound **5** was crystallized by vapor diffusion of diethyl ether or *n*-pentane into toluene. It crystallizes in the monoclinic space group $P2_1/c$ (systematic absences $0k0$, k = odd and $h0l$, l = odd) with a = 17.098(2) Å, b = 11.4592(9) Å, c = 21.096(2) Å, β = 113.539(2)°, V = 3789.3(6) Å^3, Z = 4, and d_{calcd} = 1.283 g/cm^3. X-ray intensity data were collected on a Rigaku Mercury CCD area detector employing graphite-monochromated Mo Kα radiation (λ = 0.71073 Å) at a temperature of −130 °C. Preliminary indexing was performed from a series of twelve 0.5° rotation images with exposures of 30 s. A total of 336 rotation images were collected with a crystal to detector distance of 35 mm, a 2θ swing angle of −12°, rotation widths of 0.5°, and exposures of 10 s: scan 1 was a ϕ scan from 170 to 338° at ω = 0° and χ = 0°. Rotation images were processed using CrystalClear,[67] producing a listing of unaveraged F^2 and $\sigma(F^2)$ values which were then passed to the CrystalStructure[68] program package for further processing and structure solution on a Dell Pentium III computer. A total of 15 571 reflections were measured over the ranges $5.20° \le 2\theta \le 50.02°$, $-16 \le h \le 20$, $-13 \le k \le 12$, and $-23 \le l \le 25$, yielding 6 601 unique reflections (R_{int}=0.0261). The intensity data were corrected for Lorentz and polarization effects and for absorption using REQAB[69] (minimum and maximum transmission 0.853, 1.000).

The structure was solved by direct methods (SIR97).[70] Refinement was by full-matrix least squares based on F^2 using SHELXL-97.[71] All reflections were used during refinement (F^2 values that were experimentally negative were replaced by F^2 = 0). The weighting scheme used was $w = 1/[\sigma^2(F_o^2) + 0.0547P^2 + 0.9350P]$ where $P = (F_o^2 + 2F_c^2)/3$. Non-hydrogen atoms were refined anisotropically, and hydrogen atoms were refined using a "riding" model. Refinement converged to R_1 = 0.0479 and wR_2 = 0.1107 for 5502 reflections for which $F > 4\sigma(F)$ and R_1 = 0.0599, wR_2 = 0.1204, and GOF = 1.078 for all 6 601 unique, nonzero reflections and 500 variables ($R_1 = \sum||F_o| - |F_c||/\sum|F_o|$; $wR_2 = \{\sum w(F_o^2 - F_c^2)^2/\sum w(F_o^2)^2\}^{1/2}$; GOF = $\{\sum w(F_o^2 - F_c^2)^2/(n-p)\}^{1/2}$ where n = the number of reflections and p = the number of parameters refined). The maximum Δ/σ in the final cycle of least squares was 0.001, and the two most prominent peaks in the final difference Fourier were +0.173 and −0.253 e/Å^3.

Calculating from ^{1}H VT-NMR Data the Energy Barrier for *p*-Phenylene Rotation. Equation 1 was used to determine the *p*-phenylene rotation rate at the coalescence temperature:

$$k = \frac{\pi \Delta v_0}{\sqrt{2}} \quad (1)$$

where k is the rate coefficient and $\Delta v_0 = v_A - v_B$ is the chemical shift difference (in Hz) between the two separate signals at slow

(66) van Strijdonck, G. P. F.; van Haare, J. A. E. H.; Hönen, P. J. M.; van den Schoor, R. C. G. M.; Feiters, M. C.; van der Linden, J. G. M.; Steggerdab, J. J.; Nolte, R. J. M. *J. Chem. Soc., Dalton Trans.* **1997**, 449–461.

(67) *CrystalClear*; Rigaku Corp., **1999**.

(68) *CrystalStructure*; Rigaku Corp., **2002**.

(69) Jacobsen, R. A., REQAB4 (personal communication).

(70) Altomare, A.; Burla, M.; Camalli, M.; Cascarano, G.; Giacovazzo, C.; Guagliardi, A.; Moliterni, A.; Polidori, G.; Spagn, R. *J. Appl. Crystallogr.* **1999**, *32*, 115–119.

(71) Sheldrick, G. M. *Program for the Refinement of Crystal Structures*; University of Göttingen, Göttingen, Germany, **1997**.

exchange (in this case at −93 °C or 180 K). The Arrhenius equation (2) was used to determine the activation energy, E_a, at the coalescence temperature, T (in K):

$$\ln(k/\mathrm{Hz}) = -\frac{E_a}{R}\left(\frac{1}{T}\right) + \ln(A/\mathrm{Hz}) \quad (2)$$

where A is the pre-exponential factor and R is the universal gas constant.[64]

Computational Methods. All-atom MD simulations were carried out using NAMD2.[72] The internal bonded parameters were obtained from AMBER-94,[73] and the nonbonded parameters were proposed in previous studies.[74−78] Simulations were performed in the absence of solvent at 25 °C, and the temperature was controlled using Langevin dynamics with a damping coefficient of 5 ps^{-1}. The time step of the simulations was 0.5 fs. Relaxation calculations using energy minimization consist of up to 10 000 steps of the conjugate gradient algorithm as implemented in NAMD2; the energy was monitored to confirm minimization.[72]

GRASP[63] was employed to investigate a potential interior cavity within **5**. Different conformations were generated by manual rotations of the three *p*-phenylenes. The rotations were systematically performed in 10° increments using one of the crystal structures of **5** as reference. A probe radius of 1.4 Å was used for all calculations.

Acknowledgment. I.J.D. appreciates support from the DOD (No. W81XWH-04-1-0657), the NIH (No. CA110-104), the NSF (No. CHE-0840438), a Camille and Henry Dreyfus Teacher-Scholar Award, and the UPenn Chemistry Department. J.G.S. acknowledges support from the NSF (No. DMR08-32802). We thank George Furst for discussions and access to NMR instrumentation, Emily Berkeley for access to hydrogen and helium for ^{1}H NMR experiments, and Laura Spece for her early contributions to this work. Molecular structures in Figures 1, 4, and 5 were generated using PyMOL.[79]

Supporting Information Available: A CIF file giving crystallographic data for **5** and figures giving ^{1}H NMR and ^{13}C NMR spectra, NMR experiments investigating guest binding, analysis of molecular dynamics simulations, and computational modeling. This material is available free of charge via the Internet at http://pubs.acs.org.

(72) Phillips, J. C.; Braun, R.; Wang, W.; Gumbart, J.; Tajkhorshid, E.; Villa, E.; Chipot, C.; Skeel, R. D.; Kale, L.; Schulten, K. *J. Comput. Chem.* **2005**, *26*, 1781–1802.
(73) Cornell, W. D.; Cieplak, P.; Bayly, C. I.; Gould, I. R.; Merz, K. M.; Ferguson, D. M.; Spellmeyer, D. C.; Fox, T.; Caldwell, J. W.; Kollman, P. A. *J. Am. Chem. Soc.* **1995**, *117*, 5179–5197.
(74) Kirchhoff, P. D.; Bass, M. B.; Hanks, B. A.; Briggs, J. M.; Collet, A.; McCammon, J. A. *J. Am. Chem. Soc.* **1996**, *118*, 3237–3246.
(75) Kirchhoff, P. D.; Dutasta, J. P.; Collet, A.; McCammon, J. A. *J. Am. Chem. Soc.* **1997**, *119*, 8015–8022.
(76) Kirchhoff, P. D.; Dutasta, J. P.; Collet, A.; McCammon, J. A. *J. Am. Chem. Soc.* **1999**, *121*, 381–390.
(77) Potter, M. J.; Kirchhoff, P. D.; Carlson, H. A.; McCammon, J. A. *J. Comput. Chem.* **1999**, *20*, 956–970.
(78) Rizzo, R. C.; Jorgensen, W. L. *J. Am. Chem. Soc.* **1999**, *121*, 4827–4836.
(79) DeLano, W. L. *The PyMOL Molecular Graphics System*, **2002**.